Journal of Applied Polymer Science

The Influence of Solvent Properties on the Performance of Polysulfone/β-Cyclodextrin Polyurethane Mixed-Matrix Membranes

Feyisayo V. Adams,[1] Edward N. Nxumalo,[1] Rui W. M. Krause,[1] Eric M. V. Hoek,[1,2] Bhekie B. Mamba[1]

[1]Department of Applied Chemistry, University of Johannesburg, Doornfontein 2028, South Africa

[2]Department of Civil and Environmental Engineering and California NanoSystems Institute, Los Angeles, California 90095-1593

Correspondence to: B.B. Mamba (E-mail: bmamba@uj.ac.za)

ABSTRACT: This study investigates the effect of solvent properties on the structural morphology and permeation properties of polysulfone/β-cyclodextrin polyurethane (PSf/β-CDPU) mixed-matrix membranes (MMMs). The membranes were prepared by a modified phase-inversion route using four different casting solvents [dimethyl formamide (DMF), dimethyl sulfoxide (DMSO), dimethyl acetamide (DMA), and *N*-methyl-2-pyrrolidone (NMP)]. While DMSO-based membranes demonstrated particularly high permeability (ca 147 $L/m^2h.bar$), their crystallinity was low compared to MMMs prepared using DMA, DMF and NMP due to the formation of thin active layers on their surfaces. Cross-sectional morphology revealed that the MMMs have a dense top skin with finger-like inner pore structures. Membranes prepared using NMP displayed the highest hydrophilicity, porosity, and crystallinity due to the low volatility of NMP; DMF membranes exhibited superior mechanical and thermal stability due to its (DMF) high hydrogen bonding (δH) values. Thus, the morphological parameters, bulk porosity, and flux performance of MMMs have a significant inter-relationship with the solubility properties of each solvent (i.e., δH, density, volatility, solubility parameter). © 2013 Wiley Periodicals, Inc. J. Appl. Polym. Sci. 000: 000–000, 2013

KEYWORDS: membranes; morphology; blends; polyurethanes; properties and characterization

Received 5 February 2013; accepted 5 April 2013; Published online

DOI: 10.1002/app.39378

INTRODUCTION

The fabrication of membranes using nanotechnology-based techniques can potentially offer environmentally friendly, cost-effective, and high-performance membrane architectures. However, in order to fully understand the separation performance of nanostructured membranes, it is particularly important to understand their formation processes, mechanistic phenomena as well as the polymer-solvent interactions that take place during the synthetic processes.

The phase-inversion method has been generally defined as the most reliable technique for preparing or modifying asymmetric membranes.[1] This method employs a ternary system of a polymer in a mixture of a solvent and a nonsolvent, and can be used to produce different types of membranes including mixed-matrix membranes (MMMs). The composition and temperature of the precipitating agent can be improved or modified to obtain the desired results. Indeed, the type of phase precipitation process responsible for membrane construction during this procedure is of great importance.

Strathmann[2] describes the difference between a vapour-phase precipitation process and the liquid-phase precipitation process. In the case of vapour-phase precipitation the rate-limiting step is the slow diffusion of precipitant (e.g., water vapour) from the vapour phase to the polymer solution. Since this is a relatively slow process, precipitation of the polymer is also slow, resulting in fairly large pores in the membrane. Liquid-phase precipitation is described as bringing water in contact with the polymer solution under supersaturated conditions.

Solvent-polymer and nonsolvent-polymer interactions thus play a significant role in the properties and type of the resulting membrane.[1,3] It is known that these interactions increase with increasing polymer concentration while reducing the coagulation degree or the dissolving power of the solvent.[4] While, these properties usually enhance the delay in demixing, they increase the interactions of solvent and nonsolvent that hinder diffusional exchange between solvent and nonsolvent thereby stimulating delayed demixing.[5]

Furthermore, the properties of the solvent used during the membrane-casting process have impact on the membrane morphology and separation performance.[4] For example, the addition of a volatile solvent to a nonsolvent can alter liquid–liquid interactions and result in diverse morphological architectures.[6]

Table I. Solvents Properties[11]

Type of solvent/ properties	DMA	NMP	DMF	DMSO
Density (g/cm^3)	0.94	1.03	0.95	1.10
Boiling point (°C)	166.00	202.00	153.00	189.00
Molecular weight (g/mol)	87.12	99.13	73.00	78.13
Solubility parameter (cal$^{1/2}$ cm$^{3/2}$)	10.80	8.80	12.10	13.00
Hydrogen bonding (δH)	5.00	3.50	5.50	5.00

However, the addition of a cosolvent to a polymeric solution can eliminate macrovoid formation during instantaneous demixing, and therefore the morphology of the membrane can be altered from a finger-like to a sponge-like structure.[7] It is generally known that the skin layer can either be thick or thin, porous or nonporous, while the structure beneath the skin layer can be classified as finger-like and sponge-like structures. The finger-like structures can be straight or slanting. A finger-like structure is likely to be less resistant to pressure and the membrane selectivity will, however, not be affected, while membranes with a sponge-like structure provide good permeabilities.[8]

During the phase-inversion process, a more volatile solvent is often introduced to the polymer solution to adjust the solvent evaporation and polymer coagulation in the nonsolvent (water).[9] The most common water-miscible solvents used in hydrophobic asymmetric membrane preparation processes are tetrahydrofuran (THF), acetone, dimethyl formamide (DMF), dimethyl sulfoxide (DMSO), *N*-methyl-2-pyrrolidone (NMP), and dimethyl acetamide (DMA).[10] A good water-miscible solvent exhibits a high degree of polarity and hydrogen bonding which is able to suppress the solvent volatility.[9] Hence, the outermost surface of the membrane generates high polymer concentration as a more volatile solvent is removed during the evaporation process. The more cosolvent evaporated, the thicker the concentrated polymer region which then leads to a thicker selective skin and a reduction in permeation rate.[5] The properties of the casting solvent that can potentially affect the performance of a membrane are presented in Table I.

Recently, Teow et al.[12] prepared polyvinyl difluoride (PVDF)/TiO_2 MMMs using NMP, DMA and DMF as solvents. The DMA-based membranes demonstrated better permeability with improved humic-acid retention (>98.28%) due to narrow internal pores. Polyethersulfone membranes prepared from DMF and NMP exhibited excellent retention of charged compounds as well as high permeate fluxes due to a thinner top layer formed on the membrane surface.[13] Şener et al.[14] investigated the effect of solvent type on the morphology and performance of zeolite-filled composite membranes and found that membranes prepared from DMSO had high flux and selectivity due to the higher boiling point of DMSO.

Mohammadi et al.[15] studied the separation of methanol/methyl tertiary butyl ether using cellulose acetate membranes prepared from acetone, DMF and NMP and revealed that the membranes prepared using DMF exhibited the highest selectivity and lowest flux. The difference in membranes performance was attributed to volatility differences and the evaporation rate of the solvents.

While solvent properties are significant in determining the properties and separation performances of membranes obtained using the phase-inversion technique, data are still lacking to fully understand the role of solvents in polymer/cyclodextrins MMM preparation. Therefore, it is difficult to gain an understanding of the influence of the solvent on membrane properties. Due to the complexity of solvent-polymer interactions in the reactions which differ in each type of polymer and solvent for a specific membrane type, it is difficult to accurately predict solubility behaviour. A controlled system is often needed to facilitate the accurate prediction of complex solvent-polymer interactions. In order to gain an understanding of the solvent-polymer interaction, solubility maps or graphs are often required.

Recently, Baruah et al.[16] studied the effect of solvents on the morphology of polysulfone/α-CD composite nanofiltration (NF) membranes. This work demonstrated that NMP, DMF, and DMA exhibit similar effects on the morphology and physicochemical properties of the membranes. This was explained in terms of the demixing behaviour of polysulfone (PSf) and the combined effect of solvent volatility and polymer–solvent interactions as obtained when using Hansen-solubility parameters. However, other fundamental properties such as mechanical strength and rejection efficiency were not investigated in this study. Evidently, CDs differ in physical and chemical properties to polymeric forms of CDs; previous studies demonstrate that polymeric *β*-CD/membranes have unique permeation properties.[17]

Our previous work investigated the general chemistry, thermal properties, morphology, and membrane efficiency in cadmium and glucose removal from water and the strength of these polymeric *β*-CD membranes.[17,18] Further studies were carried out on the structural properties and the transport phenomena of the membranes.[18] The objective of this work is to investigate the role of solvent properties on the characteristics of PSf/*β*-CDPU mixed-matrix NF membranes prepared using DMA, DMF, DMSO, and NMP. The solvent properties were correlated to thermal and mechanical stability, crystallinity, hydrophilicity, permeability, and atrazine rejection.

EXPERIMENTAL

Materials

Polysulfone was obtained from Solvay Advanced Polymers LLC (South Africa). All the organic solvents used in this work (DMF, DMA, DMSO, and NMP) were obtained from Sigma Aldrich. Deionised water was used as a precipitating "nonsolvent." Dibutyl tin dilaurate [DBTDL (Thorcat 401)] and hexamethylene diisocyanate (HMDI) used during the polymerisation of *β*-CD

were obtained from Merck and used without any further purification.

Preparation of β-CD Polyurethane

Hexamethylene diisocyanate (HMDI) (0.7 mL, 4.4 mmol) was added drop-wise to a solution of β-CD (5.0 g, 4.4 mmol) in DMF (50 mL). Dibutyl tin dilaurate (DBTDL (Thorcat 401) (2 mL) was then added under an inert atmosphere at room temperature (RT) and the reaction was allowed to proceed for 30 min. The polymer formed was precipitated in acetone and washed several times with acetone to remove residual DMF followed by drying at room temperature.[17]

Preparation of PSf/β-CD Polyurethane Membranes

β-CDPU (5 wt % of total polymer in solvent) and PSf were dissolved in different solvents (DMF, DMA, DMSO and NMP) under magnetic stirring whilst heating at 80°C for 2 h to achieve the desired concentration (20 wt % polymer in solvents). The homogeneous solution obtained was kept in a desiccator overnight to allow the product to settle and to remove air-bubbles formed during the reaction.

Membranes were cast on a glass plate in a uniform thickness of 200 μm using a casting knife (Elcometer 3545 Casting Knife Film Applicator). The casting knife was placed on one edge of the glass and the casting solution was slowly poured on the near end of the glass (closer to the casting knife). This was done such that no air-bubbles were trapped in the casting solution to avoid creation of holes in the membranes. The casting knife was then pulled over the casting solution to coat the glass surface. The glass coated with a wet polymer solution was left to air-dry for 60 s. This was followed by dipping the cast membranes into a nonsolvent bath of deionised water first at 4°C for 30 min and subsequently dipped into deionised water at room temperature (20°C). The newly produced membrane was allowed to dry at RT and was then sandwiched between plain sheets of paper for storage.

Characterization of PSf/β-CD Polyurethane Membranes

Fourier transform-infrared (FT-IR) spectra were collected on a Perkin Elmer 100 Spectrometer and were recorded with characteristic peaks in wave numbers from 650 cm^{-1} to 4000 cm^{-1}. The crystallinity of the MMMs was examined using a Philips PANalytical X'pert Diffractometer. X-ray diffraction (XRD) analysis was performed at 40 mA, 40 keV, Cu Kα radiation (λ = 0.1540562 nm), divergence slit of 1/8°, anti-scatter slits of 1/4°, 5 mm, over a range of 4° to 80° on the 2θ scale, without a monochromator.

A Perkin Elmer thermogravimetric analysis instrument with a heating rate of 10°C/min was used to determine the degradation pathways of membranes over a temperature range of 30°C to 800°C in nitrogen gas. The tensile strength was measured by a tensile test machine (Instron 5966) with a load cell of 10 kN at a cross-head speed of 1 mm/min and a clamp distance of 25 mm. Membrane samples with dimensions of 11 mm wide and 25 mm long were clamped between two holders. Dynamic mechanical data were obtained with a Perkin-Elmer DMA instrument. All samples were tested within the temperature range of 60°C to 250°C at a heating rate of 5°C/min and a clamp mass of 5.66 g, strain factor of 19.2 and a frequency of 1 Hz were selected for all the experiments. The discrete displacement amplitude value was 0.02 mm. The morphology and the cross-section of the membranes were viewed by mounting samples on a high-resolution scanning electron microscope (HRSEM) [NOVA NanoSEM 200 (FEI) scanning microscope] and irradiating them with a beam of electrons at 10 KV. This was followed by proper magnification and precise focusing for better viewing of the specimen's surface. A Data Physics OCA (optical contact angle) measuring instrument was used to measure water-contact angles with the droplet size controlled by a Gilmont syringe. Water droplets (deionised water) were contacted with the membrane at about nine different locations on each membrane sample to obtain a series of contact-angle pairs. All measurements were carried out at RT.

Swellability was determined by taking the weight difference before and after immersion in water. The membranes were soaked in deionised water for a period of 24 h, then wiped with blotting paper to remove excess water, and thereafter weighed to obtain the wet weight. The dry weights were obtained after drying the wet samples in an oven at 80°C for 24 h. The percentage of water uptake was then obtained using eq. (1):

$$\text{Water content} = \frac{W_0 - W_1}{W_0} \times 100 \quad (1)$$

where W_0 and W_1 are the weights of wet and dry membranes (measured in g), respectively.

The bulk porosity of membranes (P) was further determined using the following equation:

$$P(\%) = \frac{W_0 - W_1/\rho_w}{Ah} \times 100 \quad (2)$$

where A is the membrane surface area (cm^2), ρ_w is the density of water (g/cm^3), and h is the membrane thickness (mm).

Membrane performance was determined from pure water-permeability measurements, and atrazine rejections (25 mg/L) at RT using a Sterlitech dead-end filtration cell at a pressure of 0.50 MPa using nitrogen gas. Acetone was used for atrazine solution preparation. The water permeability (J_w) was determined by using eq. (3).

$$J_w = \frac{V}{APt} \quad (3)$$

where V is the permeate volume (l), A is the membrane effective area (0.00146 m^2), t is the time (h) necessary for the permeate volume to be collected, and P is the applied pressure (MPa).

To evaluate the membranes' efficiency in removing atrazine from the feed solution, the rejection (R) was used and it is defined as:

$$R(\%) = \frac{C_f - C_p}{C_f} \times 100 \quad (4)$$

where C_f denotes atrazine concentration in the feed (mg/m^3) and C_p denotes atrazine concentration in the permeate (mg/m^3).

RESULTS AND DISCUSSION

FT-IR Analysis

Figure 1 depicts the FT-IR spectra of PSf/β-CDPU membranes prepared from various casting solvents. The bands associated

Applied Polymer SCIENCE

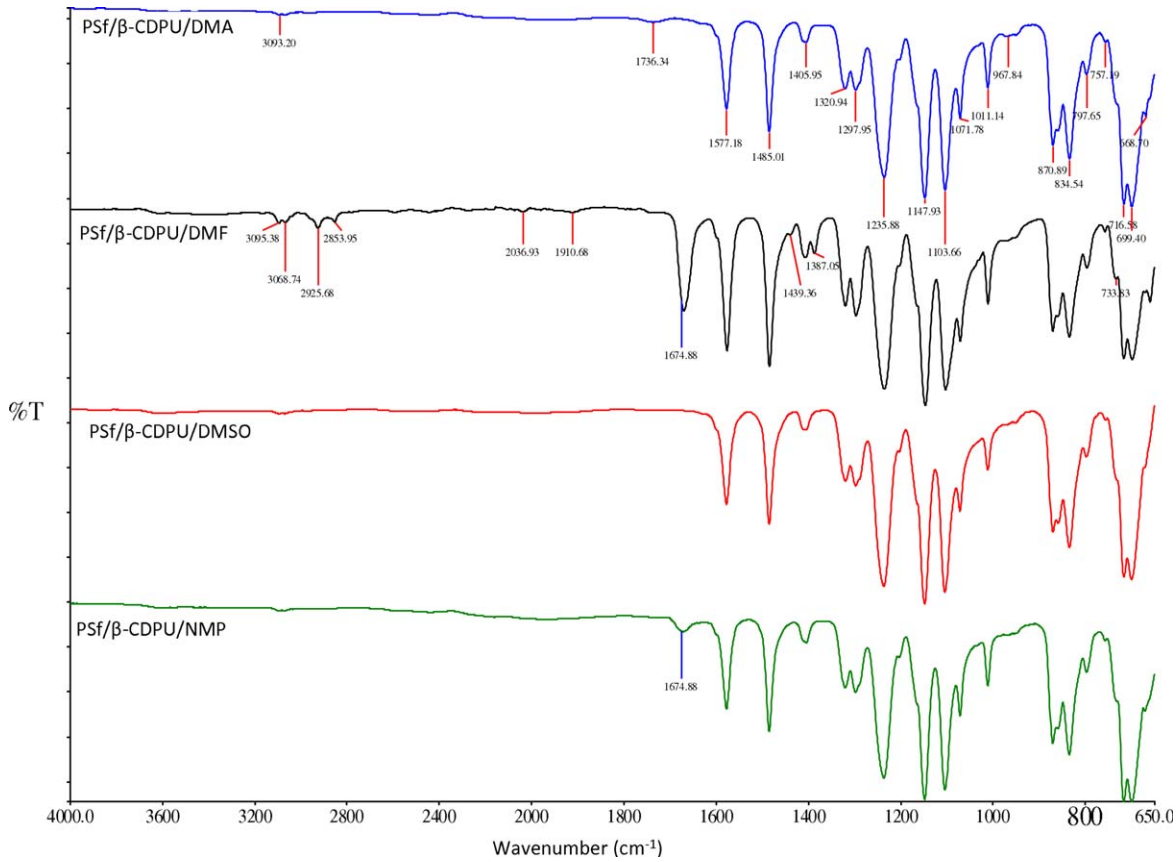

Figure 1. FT-IR spectra of the membranes prepared from different solvents. [Color figure can be viewed in the online issue, which is available at wileyonlinelibrary.com]

with aromatic —CH vibrations were found at ~3094 cm^{-1} and 3067 cm^{-1}. The band located at 2924 cm^{-1} corresponds to —CH stretching absorption while the peak at 2852 cm^{-1} is ascribed to aliphatic —CH_2 asymmetric stretching. This observation is in agreement with results published by Baruah et al.[16] The band found at 1668 cm^{-1} was assigned to —C—C benzene deformation bands. The benzene deformation band is applicable to the membranes prepared from DMF, (PSf/β-CDPU/DMF), DMSO (PSf/β-CDPU/DMSO) and NMP (PSf/β-CDPU/NMP). The intense peak in the PSf/β-CDPU/DMF membranes is due to strong H-bonding forces which consequently result in significant differences in the properties of membranes prepared using the various solvents. The —SO_2 and —C—O stretches found in the range of 1000 cm^{-1} to 350 cm^{-1} are characteristic of PSf membranes.[16] The -OH peak which is a characteristic of β-CDPU is absent in all the membranes due to solvent-polymer interactions and low β-CDPU concentration in the doping solution. The characterisation of β-CDPU itself was not discussed in this work: data is already published. [17]

Thermogravimetric Analysis

Figure 2 shows TGA profiles of the various MMMs. The PSf/β-CDPU/DMF membranes show a five-step decomposition process while membranes prepared from DMA (PSf/β-CDPU/DMA) and PSf/β-CDPU/NMP membranes show four-step decomposition. PSf/β-CDPU/DMSO membranes show a three-step decomposition process. The decomposition steps were initially slow between temperatures of 30°C and 170°C due to the loss of water. The weight loss between 160°C and 340°C is attributed to the loss of residual solvents. The decomposition temperatures for PSf/β-CDPU/DMA, PSf/β-CDPU/NMP and PSf/β-CDPU/DMSO membranes were < 600°C, whereas the decomposition temperatures of the PSf/β-CDPU/DMF membranes were > 600°C. Complete decomposition was reached at 573°C, 564°C, 564°C, and 648°C for PSf/β-CDPU/NMP, PSf/β-CDPU/DMA, PSf/β-CDPU/DMSO, and PSf/β-CDPU/DMF membranes, respectively. It is evident that PSf/β-CDPU/DMF membranes are more thermally stable than PSf/β-CDPU/DMA, PSf/β-CDPU/DMSO, and PSf/β-CDPU/NMP membranes (Figure 2). The total weight loss observed for the PSf/β-CDPU/DMF membranes was high (ca 96%). However, the total weight losses of PSf/β-CDPU/DMA, PSf/β-CDPU/DMSO, and PSf/β-CDPU/NMP membranes were found to be 59.50%, 59.90%, and 59.20%, respectively. The variation in the weight loss of the membranes is observed to be directly proportional to the molecular weight of the solvents (see Table I).

Membrane Crystallinity

X-ray diffraction (XRD) results illustrating the effect of solvents on the crystalline structure of MMMs are shown in Figure 3. The results show that the intensity of the crystalline peak of the membranes decreased with an increase in density and solubility

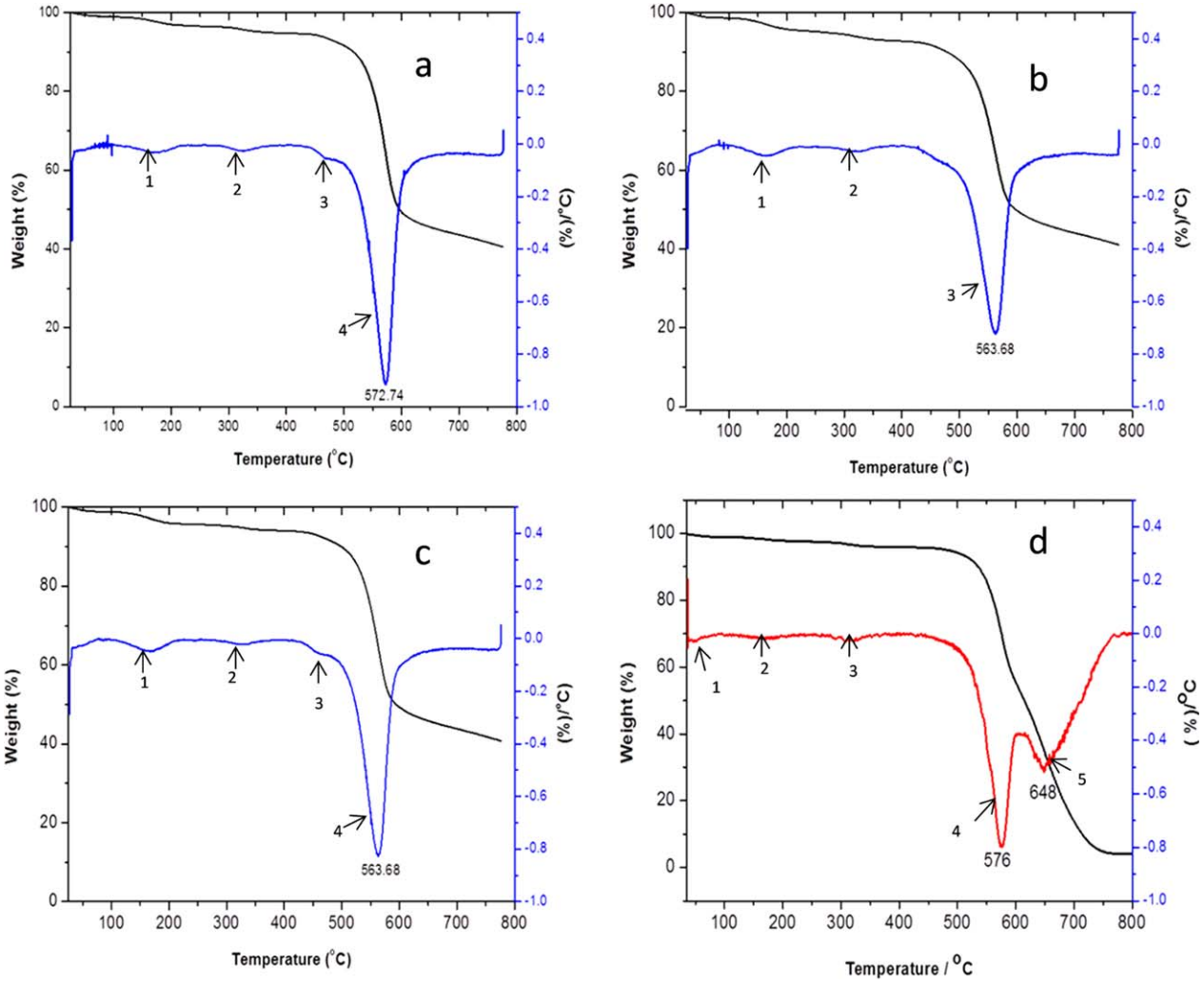

Figure 2. TGA spectra of (a) PSf/β-CDPU/NMP membrane; (b) PSf/β-CDPU/DMSO membrane; (c) PSf/β-CDPU/DMA membrane; and (d) PSf/β-CDPU/DMF membrane. *Note: 1,2,3,4 and 5 represent each decomposition step. [Color figure can be viewed in the online issue, which is available at wileyonlinelibrary.com]

parameter of the solvents.[12] Thus, the PSf/β-CDPU/NMP membranes exhibited the highest crystallinity. A reduction in the impermeable crystalline phase and subsequent increase in the permeable amorphous matrix can result in free volume.[19] Since solvent and solute are expected to permeate through the free volume between the segments of the PSf/β-CDPU polymer it is expected that the pure water permeability through these membranes will follow the trend: PSf/β-CDPU/NMP < PSf/β-CDPU/DMA < PSf/β-CDPU/DMF < PSf/β-CDPU/DMSO. However, other parameters such as porosity and hydrophilicity can influence membrane permeability.

Contact Angle, Bulk Porosity, and Swellability

Table II shows the contact angles, bulk porosity and water uptake obtained for the mixed-matrix composite membranes synthesised. The data demonstrates that the performance of MMMs generally depends on the hydrophobicity of the casting solvent. The contact angles of a membrane reflect its wettability and can be related to its swellability. DMSO is known to be the most polar solvent and thus it was expected to produce membranes with higher hydrophilicity. High wettability means high hydrophilicity which indicates that there is a high interaction between the membrane surface and the water molecule. However, due to the low chemical interaction between DMSO and PSf these membranes were found to be more hydrophobic. The PSf/β-CDPU/NMP membranes were found to be more hydrophilic due to the chemical interactions between the polymer composite and the solvent (i.e. H-bonding with the SO_2 moiety of the PSf backbone). Similar observations were made by Baruah et al.[16] where α-CD-NMP membranes exhibited lower contact angles (38°) while α-CD-DMSO membranes exhibited higher contact angles (57°). This interaction was as a result of low residual solvent removal during coagulation. The remaining solvent gave rise to low contact angles.

The bulk porosity and the water uptake of membranes decreased with an increase in δH values of the solvents. Additional nitrogen atoms (nitrile group) present in the PSf/β-

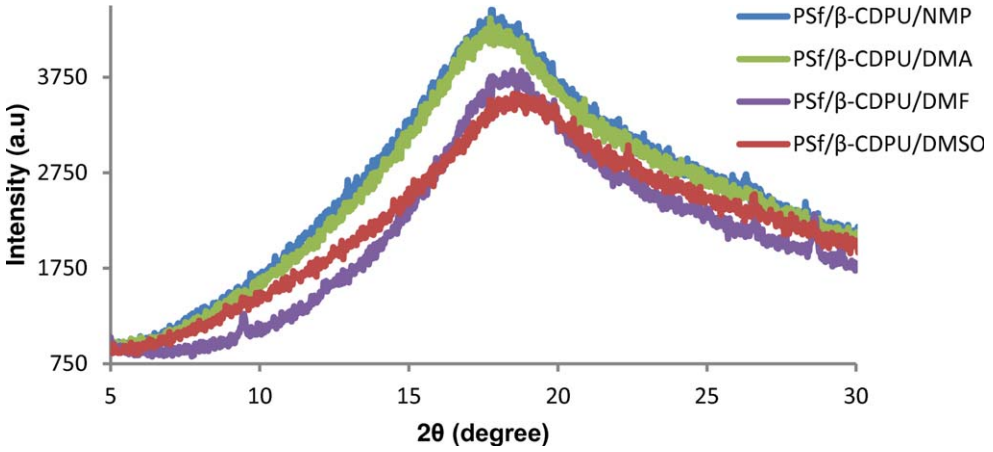

Figure 3. XRD of the membranes prepared from different solvents. [Color figure can be viewed in the online issue, which is available at wileyonlinelibrary.com]

CDPU/NMP membranes also contributed to N-O bonding resulting in higher porosities. These nitrile groups have high δH values and can easily interact with water molecules, consequently leading to lower contact angles.[20] According to Semenova et al.,[20] carbonyl groups (C=O) and imide (NH-) groups can easily form H-bonding with water. Thus, the nitrile groups which are included in the side-chain of the surface of the PSf/β-CDPU/NMP membranes form hydrogen bonds with water rendering them more hydrophilic.

Tensile Strength Tests

Table III shows the results obtained from the mechanical tensile strength of the membranes. The results revealed that PSf/β-CDPU/DMF membranes displayed higher ultimate tensile strength (UTS: 7.1 MPa) compared to the other MMMs. The UTS values for PSf/β-CDPU/DMA, PSf/β-CDPU/NMP, and PSf/β-CDPU/DMSO membranes were 5.2 MPa, 4.6 MPa, and 7.0 MPa, respectively. The results obtained show that δH of the solvents (relative to PSf/β-CDPU used in membrane preparation) influenced UTS results. An increase in δH values results in an increase in UTS values and therefore in the overall strength of the MMMs. This is expected since it is known that membranes with macrovoids often have inferior mechanical properties.[7,21] Tsai et al.[7] reported a substantial decrease in the mechanical strength of membranes containing the surfactant Tween-20 due to weak spots which can induce macrovoid formation in the porous skin layer. However, the results presented in the present study suggest that this is not the case with PSf/β-CDPU/DMSO membranes. The cross-sectional morphology shows that DMSO forms membranes with macrovoids in the sub-layers. Nonetheless, these membranes exhibited better strength compared to the PSf/β-CDPU/DMA and PSf/β-CDPU/NMP membranes which have fewer macrovoids in the sub-layers. Contrary to these findings, Arthanareeswaran and Starov[22] observed that membranes prepared using PES/NMP were more mechanically stable compared to membranes prepared using DMF and DMSO. This was as a result of the decrease in the thickness of the top active porous layer and the rapid diffusion rate of DMF and DMSO in the polymer matrix.

It is now known that different functional groups on a polymer provide the polymer ionic bonding or H-bonding between its own chains.[20] These stronger forces typically result in higher tensile strength and higher crystalline melting points. The partially positively charged hydrogen atoms in the -N-H groups (solvent) of one chain are strongly attracted to the partially negatively charged oxygen atoms in the —C═O groups (β-CDPU). A similar trend was observed for the tensile modulus values: an increase in δH results in an increase in the tensile modulus of the membrane. This results in lower permeabilities.

Dynamic Mechanical Analysis

Figures 4 and 5 show the tan δ and modulus curves for the dynamic mechanical behaviour of PSf/β-CDPU in different solvents and in the temperature range of 60°C to 250°C. PSf/β-

Table II. Contact Angle, Porosity, and Water Uptake of Membranes Prepared from Different Solvents

Type of membrane	Contact angle (°)	Porosity (%)	Water uptake (%)
PSf/β-CDPU/DMA	42 ± 1.2	9	44
PSf/β-CDPU/DMF	49 ± 3.1	6	28
PSf/β-CDPU/DMSO	54 ± 0.6	7	34
PSf/β-CDPU/DMA	28 ± 0.6	13	46

Table III. Tensile Strength Data of Membranes Prepared from Different Solvents

Type of membrane	Modulus (MPa)	UTS (MPa)	Tensile strain (%)	Stress at tensile strength (MPa)
PSf/β-CDPU/NMP	163	4.6	5.1	5.1 ± 2.96
PSf/β-CDPU/DMF	246	7.1	20.8	7.1 ± 0.47
PSf/β-CDPU/DMSO	235	7.0	7.0	6.9 ± 0.57
PSf/β-CDPU/DMA	186	5.2	7.2	6.1 ± 0.16

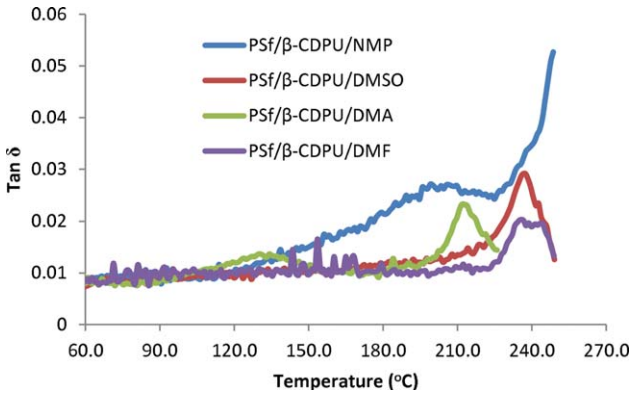

Figure 4. Tan δ curves of the membranes prepared from different solvents. [Color figure can be viewed in the online issue, which is available at wileyonlinelibrary.com]

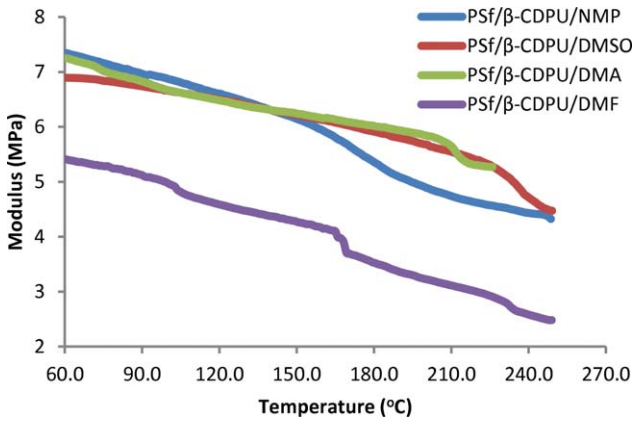

Figure 5. Young moduli curves of the membranes prepared from different solvents. [Color figure can be viewed in the online issue, which is available at wileyonlinelibrary.com]

CDPU/DMA membranes showed two major peaks, one at 128°C (weaker) and one at 211°C, (more distinct). However, PSf/β-CDPU/DMF, PSf/β-CDPU/DMSO, and PSf/β-CDPU/NMP membranes showed only one peak. It was observed that the PSf/β-CDPU/DMA membranes distorted at a temperature of below 250°C while the PSf/β-CDPU/DMF, PSf/β-CDPU/NMP, and PSf/β-CDPU/DMSO membranes

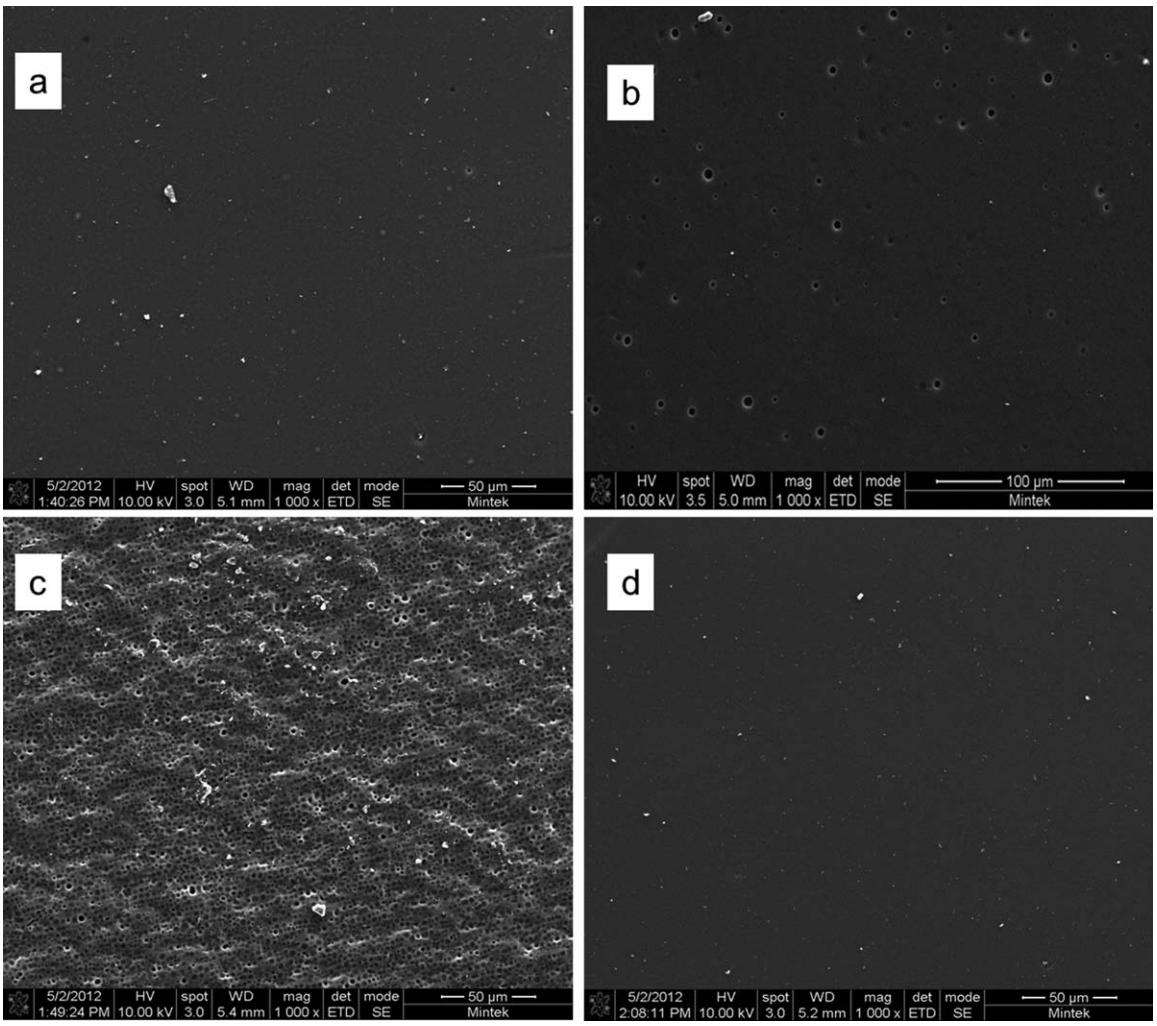

Figure 6. Surface morphology of (a) PSf/β-CDPU/DMA membrane; (b) PSf/β-CDPU/DMF membrane; (c) PSf/β-CDPU/DMSO membrane; and (d) PSf/β-CDPU/NMP membrane.

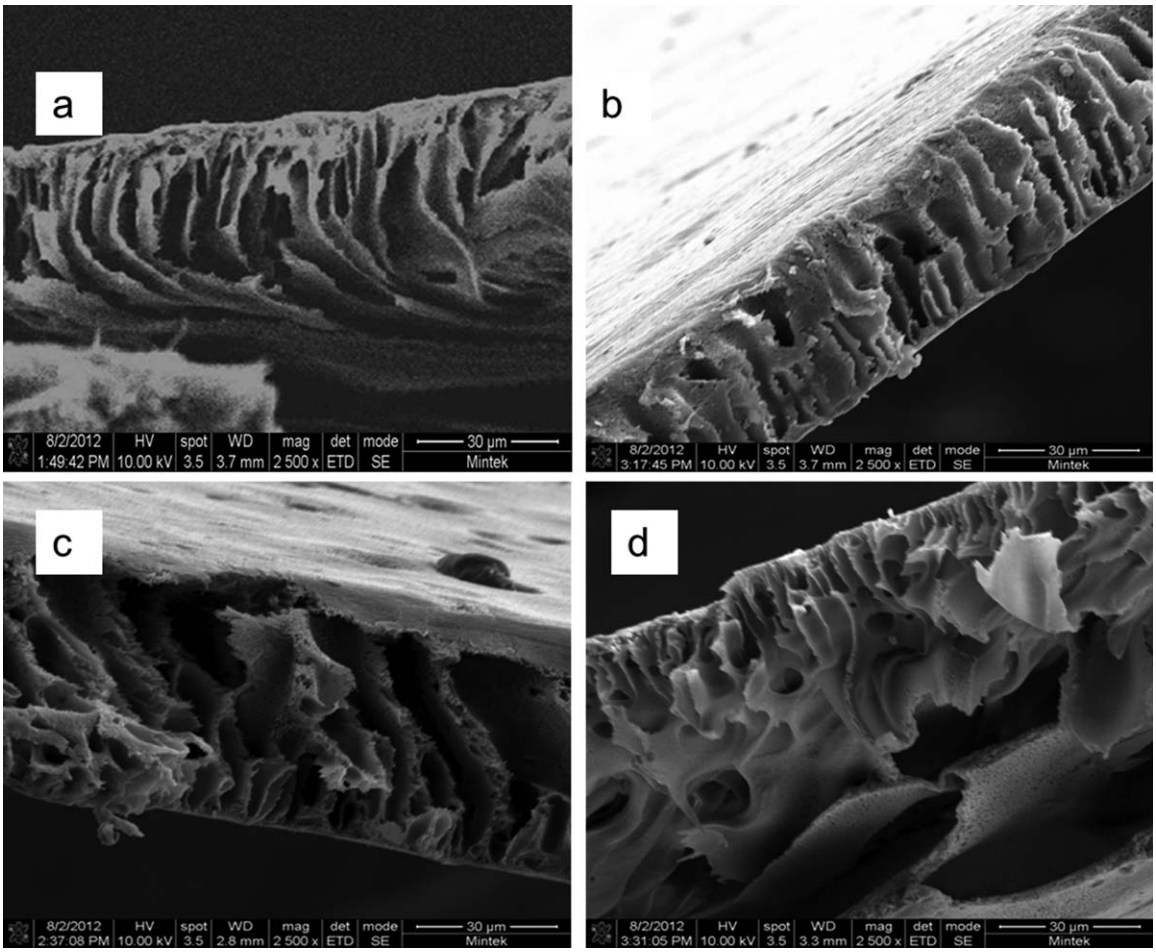

Figure 7. Cross-section images of (a) PSf/β-CDPU/DMA membrane; (b) PSf/β-CDPU/DMF membrane; (c) PSf/β-CDPU/DMSO membrane; and (d) PSf/β-CDPU/NMP membrane.

reached a temperature of 250°C without distortion. This results thus show that PSf/β-CDPU/NMP membranes maintained their structural integrity, even at temperatures > 250°C.

Generally, the Young's moduli of the membranes were found to decrease with an increase in temperature. At a temperature of 136°C, PSf/β-CDPU/DMA, PSf/β-CDPU/NMP, and PSf/β-CDPU/DMSO membranes displayed a similar Young's modulus of *ca* 6.34 MPa. At a temperature of below 100°C, PSf/β-CDPU/NMP membranes exhibited the highest modulus, while the PSf/β-CDPU/DMF membranes exhibited the lowest modulus. Clearly, the strength and stiffness of these membranes depend on the δH and crystallinity of the solvents used during preparation, especially at lower temperatures. The T_g values were observed to be 237°C, 236°C, 210°C, and 196°C for PSf/β-CDPU/DMF, PSf/β-CDPU/DMSO, PSf/β-CDPU/DMA, and PSf/β-CDPU/NMP membranes, respectively.

SEM Observations

The SEM micrographs of the top surface (air side) and cross-section of the MMMs are presented in Figures 6 and 7. In general, the surface morphology of the membranes showed that the membrane surface had fine pore structures. The circular and dark large voids on the surface of PSf/β-CDPU/DMSO membranes are nonuniform and more in number while those observed on PSf/β-CDPU/DMF membranes are more uniform (however few). However, PSf/β-CDPU/DMA and PSf/β-CDPU/NMP membranes show smaller and fewer dark voids. The morphology and separation properties of a membrane can be predicted by the amount of time it takes for phase separation to be initiated. Typically, precipitation initiated immediately after immersion results in a membrane with a porous top layer. However, precipitation that starts after a delayed time (the so-called delayed precipitation) leads to a membrane with a dense skin layer.[23–25] Further, solvent volatility and solvent-polymer interaction play a vital role in the resulting membrane morphology. More volatile solvents such as DMF and DMSO evaporate faster than NMP and DMA and this rapid evaporation can result in the formation of grainy and irregular structures. In addition, an exothermic reaction was observed when PSf/β-CDPU/DMSO membranes were immersed in water. The rapid evolvement of DMSO resulted in the formation of larger pore sizes. The membrane pore formation depends on the solvent volatility (the higher the volatility the larger the pore sizes); thus PSf/β-CDPU/DMSO membranes exhibit larger pores.

The cross-sectional images of the PSf/β-CDPU/DMSO membranes show a dense top layer on the surface (Figure 7). This

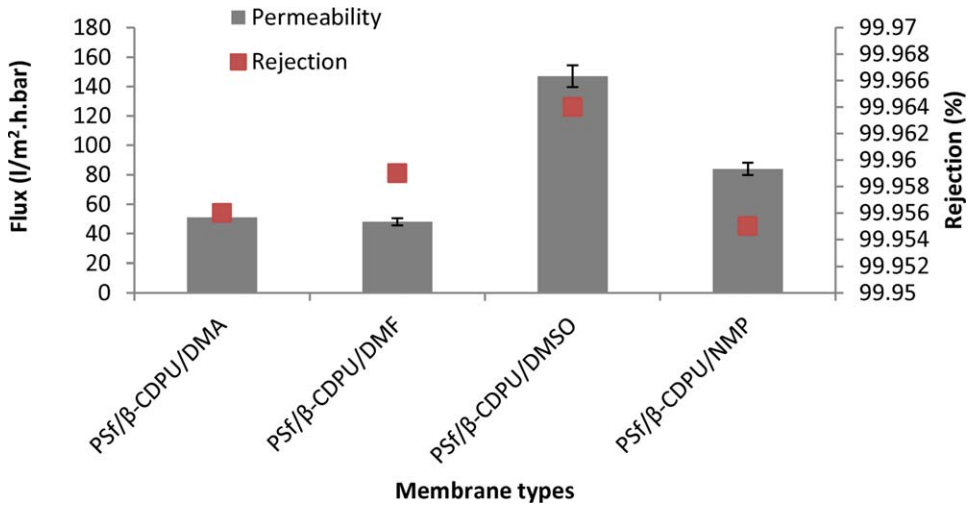

Figure 8. Permeability and rejection tests results of the membranes prepared from different solvents. [Color figure can be viewed in the online issue, which is available at wileyonlinelibrary.com]

was as a result of a high affinity of DMSO for water molecules (i.e. DMSO solubility in water). All the membranes produced in this study exhibited finger-like inner pore structures. These characteristic finger-like structures were continuous for PSf/β-CDPU/DMA, PSf/β-CDPU/DMF, and PSf/β-CDPU/DMSO membranes. However, the PSf/β-CDPU/NMP membranes showed a unique microstructure. This was as a result of a slower demixing that occurred during coagulation. The observation made in this study differs from findings reported by Baruah et al.[16] where various solvents produced membranes (α-CD-NMP, α-CD-DMSO, α-CD-DMA, and α-CD-DMF) with sponge-like structures.

Membrane Separation Performance

Permeability results show that permeability increased with an increase in polarity index and volatility of solvents (Figure 8). The PSf/β-CDPU/DMSO membranes exhibited the highest permeability and PSf/β-CDPU/DMF membranes showed the lowest permeability. Similar observations were made by Mohammadi et al.[15] who reported that membranes prepared using DMF exhibited lower flux (but higher selectivity) compared to membranes prepared using NMP and acetone. This performance is consistent to the solvents' volatility differences. The high permeability of the PSf/β-CDPU/DMSO membranes was due to the formation of a relatively thin active layer and macrovoids in the sub-layers. Therefore, PSf/β-CDPU/DMF membranes demonstrate lower permeability due to the thicker active layer. Arthanareeswaran and Starov[22] observed that DMSO-based membranes gives higher permeability efficiency compared to membranes prepared from DMF and NMP. In this study, amorphous membranes (PSf/β-CDPU/DMSO) allowed water to diffuse through while hydrophilic membranes (PSf/β-CDPU/MP) held back water molecules and thus slowed down the permeability.

The rejection performance of the MMMs in different solvents is in the order of PSf/β-CDPU/DMSO > PSf/β-CDPU/DMF > PSf/β-CDPU/DMA > PSf/β-CDPU/NMP membranes, which show that rejection increases according to an increase in solubility parameter of the solvents. Similarly, Şener et al.[14] reported that DMSO-based membranes exhibit outstanding performance in terms of selectivity and permeability. However, the authors suggested that higher boiling point and solubility of DMSO were responsible for this performance.

Solvent Effect Perspectives

The solubility parameter of solvents in water and solvent boiling point has an effect on the performance of membranes. Concurrently, the membrane performance depends on the structural properties and morphology of the membrane. It has been reported that the inter-diffusion rate of solvent-nonsolvent (solvent-water) depends on the value of Hansen solubility parameters of the solvent and that of the nonsolvent.[14] On the other hand, the solvent-nonsolvent interaction is a determinant of the type of pore structure formed during the phase-inversion process, which further determines the overall performance of the membranes. Membranes which exhibit a porous top layer are usually formed as a result of rapid precipitation (more volatile solvents), while a membrane with a dense skin layer is formed when using delayed precipitation (less volatile solvents). Indeed, the rapid evolvement of DMSO during the phase-inversion process resulted in the formation of membranes with larger pores.

Slanting finger-like structures are obtained at lower solvent-nonsolvent interactions due to rapid solvent evaporation compared to the permeation rate of the nonsolvent into the membranes.[4] This implies that the formation of slanting finger-like structures in the PSf/β-CDPU/DMA membranes was due to a low solvent-nonsolvent interaction since DMA is less volatile compared to DMSO and DMF. According to Hasbullah et al.[26] solvent-nonsolvent interactions depend on solvent viscosity and boiling point. According to the authors, higher solvent boiling points and viscosities result in better membrane performance. Şener et al.[14] and Hasbullah et al.[26] reported that the boiling point of solvent plays a significant role in membrane preparation and performance. As a consequence, PSf/β-CDPU/DMSO membranes exhibited better performance than the other membranes that were studied.

CONCLUSION

The performance of membranes can be correlated with the membrane structural morphology and surface properties. In addition, the properties of the solvent used, i.e., boiling point, viscosity, density, etc., can affect the membrane morphology and separation performance. As a consequence, poor solvent-nonsolvent interactions (e.g. in DMA-based membranes) result in the formation of slanting finger-like structures since solvent evaporates faster than the permeation rate of nonsolvent into the membranes. Clearly, high permeability is largely dependent on the formation of a thin active layer and macrovoids in the sub-layers (DMSO-based membranes). Further, bulk porosity and water uptake of membranes depend on the δH of each solvent, e.g., nitrile groups have high δH which can easily interact with the water molecule thus leading to a lower contact angle. Casting solvents with high δH values yield membranes with enhanced mechanical strength. In addition, solvents with high boiling points and viscosities effectively promote the formation of MMMs with superior performance.

ACKNOWLEDGEMENT

The authors express their gratitude to the University of Johannesburg where this research work was carried out, the DST/Mintek Nanotechnology Innovation Centre (Water Research Platform) for funding and Solvay Advanced Polymers LLC for providing the polysulfone used in this study.

REFERENCES

1. Uekama, K. *J. Incl. Phenom. Macrocycl. Chem.* **2002**, *44*, 3.
2. Strathmann, H. Membranes Separation Processes. I. Principles. Ullmann's Encyclopedia of Industrial Chemistry; John Wiley & Sons, Ltd, Institut für chemische Verfahrenstechnik, Universität Stuttgart, Germany, 2011.
3. Farcas, A.; Jarroux, N.; Farcas, A. M.; Harabagiu, V.; Guegan, P. *Digest J. Nanomater. Biostruct.* **2006**, *1*, 55–60.
4. Ismail, A. F.; Lai, P. Y. *Sep. Purif. Technol.* **2003**, *33*, 127.
5. Sapkal, V. S.; Bansod, P. G.; Sapkal, R. S. *Int. J. Chem. Sci. Appl.* **2011**, *2*, 156.
6. Szente, L.; Szejtli, J. *Trends Food Sci. Technol.* **2004**, *15*, 137.
7. Tsai, H.-A.; Huang, D. H.; Ruaan, R. C.; Lai, J.-Y. *Ind. Eng. Chem. Res.* **2001**, *40* 5917.
8. Yu, Y.; Tim, Y.; Shi, G.; Li, J.; Chen, C. *J. Membr. Sci.* **2006**, *270*, 146.
9. Julian, H.; Wenten, I. G. *J. Eng.* **2012**, *2*, 484.
10. Pesek, S. C.; Koros, W. J. *J. Membr. Sci.* **1993**, *81*, 71.
11. Flick, E.W. Industrial Solvent Handbook, Fifth edition C.H.I.P.S., Texas/USA, **1988**.
12. Teow, Y. H.; Ahmad, A. L.; Lim, J. K.; Ooi, B. S. *Desalination* **2012**, *295*, 61.
13. Boussu, K.; Van der Bruggen, B.; Vandecasteele, C. *Desalination* **2006**, *200*, 416.
14. Şener, T.; Okumuş, E.; Gürkan, T.; Yilmaz, L. *Desalination* **2010**, *261*, 181.
15. Mohammadi, A.; Villauenga, J. P. G.; Kim, H. J.; Chan, T. *J. Appl. Polym. Sci.* **2001**, *82* 2882.
16. Baruah, K.; Hazarika, S. I.; Borthakur, S.; Dutta, N. N. *J. Appl. Polym. Sci.* **2012**, *125*, 3888.
17. Adams, F. V.; Nxumalo, E. N.; Krause, R. W. M.; Hoek, E. M. V.; Mamba, B. B. *J. Membr. Sci.* **2012**, *405*, 291.
18. Adams, F. V.; Dlamini, D. S.; Nxumalo, E. N.; Krause, R. W. M.; Hoek, E. M. V.; Mamba, B. B. *J. Membr. Sci.* **2013**, *429*, 58.
19. Hyder, M. N.; Huang, R. Y. M.; Chen, P. *J. Membr. Sci.* **2009**, *326*, 363.
20. Semenova, I. S.; Ohya, H.; Soontarapa, K. *Desalination* **1997**, *110*, 251.
21. Ogawa, H.; Kanaya, T.; Nishida, K.; Matsuba, G. *Polymer* **2008**, *49*, 245.
22. Arthanareeswaran, G.; Starov, V. M. *Desalination* **2011**, *267*, 57.
23. Wang, D. L.; Li, K.; Teo, W. K. *J. Membr. Sci.* **1995**, *98*, 233.
24. Mc Kelvey, S. A.; Clausi, D. T.; Koros, W. J. *J. Membr. Sci.* **1997**, *124*, 223.
25. Reuvers, A. J.; Van den Berg, J. W. A.; Smolders, C. A. *J. Membr. Sci.* **1987**, *34*, 45.
26. Hasbullah, H.; Ismail, A. F.; Ng, B. C.; Abdullah, M. S. International Conference on Chemical and Bioprocess Engineering in conjunction with 19th Symposiun of Malaysian Chemical Engineers, **2005**, 869.